# Polymerization Kinetics and Microstructure of Waterborne Acrylic/Alkyd Nanocomposites Synthesized by Miniemulsion

**MONIKA GOIKOETXEA, ROQUE J. MINARI, ITXASO BERISTAIN, MARÍA PAULIS, MARÍA J. BARANDIARAN, JOSÉ M. ASUA**

Institute for Polymer Materials, POLYMAT, Departamento de Química Aplicada, University of the Basque Country, Centro Joxe Mari Korta, Avenida Tolosa 72, 20018 Donostia-San Sebastián, Spain

*Received 24 March 2009; accepted 22 May 2009*
*DOI: 10.1002/pola.23535*
*Published online in Wiley InterScience (www.interscience.wiley.com).*

**ABSTRACT:** Waterborne acrylic-alkyd nanocomposites are expected to combine the positive properties of alkyd resins and acrylic polymers. In this work, the kinetics of the miniemulsion polymerization used to synthesize these nanocomposites and the effect of the process variables on the polymer architecture and particle morphology was investigated. It was found that resin hydrophobicity and the type of initiator strongly affected the microstructure of these materials. The mechanisms responsible for these effects were discussed. © 2009 Wiley Periodicals, Inc. J Polym Sci Part A: Polym Chem 47: 4871–4885, 2009

**Keywords:** alkyds; coatings; composites; emulsion polymerization

## INTRODUCTION

Traditionally, alkyds have been largely used as binders for coatings. They have good penetration, adhesion and gloss, and they can be crosslinked to achieve hardness. In addition, because of limited fossil resources, the use of alkyds, that are based on vegetable oils, a renewable source, helps to reduce the consumption of oil-based products and the dependence on the oscillating prices of crude oil.[1] However, alkyd resins are viscous tacky materials that need to be dissolved in organic solvents to be applied.

In a scenario of increasing concern for sustainability and stricter environmental legislation,[2] the demand of "solvent-free" coatings is greater than ever. Volatile organic compounds are allergic, carcinogenic, and irritant, and they are related to many environmental problems, such as the ozone formation in the troposphere. For that reason, coatings industry has switched to water-based products like acrylic latices. However, although acrylic latices offer many advantages (easy water clean-up, short drying, etc.), they still lack of the advantages of alkyds. The expectation that combination of alkyds and acrylics will result in coatings that have the good properties of both materials has been the driving force to develop waterborne alkyd/acrylic hybrids systems as binders for coatings. The improvement of properties is expected to be maximum with intimate contact of both materials. Because alkyd resin and acrylic polymer are not compatible, the challenge in this kind of materials is to compatibilize them.

Emulsion polymerization of acrylate monomers in the presence of alkyds was investigated by Nabuurs et al.[3] finding an increasing phase separation as polymerization proceeded and low final monomer conversion. Wang et al.[4] proposed the use of miniemulsion polymerization to produce

*Correspondence to:* J. M. Asua (E-mail: jm.asua@ehu.es)

Journal of Polymer Science: Part A: Polymer Chemistry, Vol. 47, 4871–4885 (2009)

these materials. Miniemulsion polymerization allows the incorporation of hydrophobic components into polymer particles because the need of mass transfer through the aqueous phase is avoided.[5–7] When alkyd resins are included in the miniemulsion formulation, they are present in the polymerization loci and by reaction of their double bonds, graft alkyd-acrylic copolymer may be formed.[8,9] This graft copolymer acts as compatibilizer between the pure acrylic and the alkyd.[10]

The grafting reaction that takes place during the polymerization process has been extensively studied.[11,12] Tsavalas et al.[13] provided a detailed explanation of the mechanisms of grafting of hybrid systems. Grafting can occur by radical addition to the alkyd carbon–carbon double bonds and by abstraction of allylic hydrogens. The addition process is energetically favored over abstraction, but the structures of the acrylic monomers and the initiators as well as the reaction conditions play an important role in determining the preferred grafting route. The chain transfer produces a relatively inactive radical on the resin, which results in a reduction in the overall polymerization rate. The practical implementation of hybrid miniemulsion polymerization is jeopardized by the relatively low limiting conversion often observed in these systems.[14] The combined role of the glass effect and the entrapment of the monomer due to the partitioning into the core-shell system[15] as well as the formation of inactive radicals on propagation of the monomeric radicals with the vinyl groups of the resin[16] have been proposed as reasons for the limiting conversion. Nevertheless, particle morphology that is expected to have a strong effect on film formation[17] has been scarcely discussed.[18,19]

The objectives of the present work are (i) to study the kinetics of the miniemulsion polymerization used to synthesize high solids waterborne acrylic-alkyd nanocomposites, which would allow determining the cause on limiting conversion and to find ways to overcome it and (ii) to study the effect of the process variables on polymer architecture and particle morphology. This knowledge will allow the synthesis of well-defined acrylic-alkyd hybrid latex.

## EXPERIMENTAL

Technical grade monomers, methyl methacrylate (MMA, Quimidroga), butyl acrylate (BA, Quimidroga), and acrylic acid (AA, Aldrich) were used without purification. Two kinds of alkyd resins were used: SETAL 293-XX (S293, acid value 11 mg KOH/g) and the more hydrophilic one SETAL 1630WP-292 (S1630, acid value 21.5 mg KOH/g), both supplied by Nuplex Resin. Both resins have similar iodine values that are proportional to the content of double bonds (S293: 118 g/100 g; S1630: 112 g/100 g). Stearyl acrylate (SA, Aldrich) was used as both monomer and costabilizer, and Dowfax 2A1 (alkyldiphenyl oxide disulfonate, Dow Chemicals) as surfactant. Water soluble initiators, (potassium persulfate, KPS, and ammonium persulfate, APS; Panreac), an organic soluble initiator, (2,2-azobis(2-methylbutyronitrile), V59, Wako Chemicals) and two water-soluble redox systems [APS/sodium metabisulfite (MBS, Panreac, molar ratio 1/1) and *tert*-butyl hydroperoxide/ascorbic acid (TBHP/AsAc, Panreac, molar ratio 2/1)] were used. Sodium bicarbonate ($NaHCO_3$, Riedel-de Haën) was used to control the miniemulsion viscosity by reducing the intense electrostatic interactions between droplets. For the hybrid polymer characterization, GPC grade tetrahydrofuran (THF, Scharlau) and diethyl ether (DEE, Sigma Aldrich) were used. Distilled water was used throughout the work.

### Miniemulsification

All miniemulsions contained 50% wt solids contents, 50% wbop (weight based on organic phase) of alkyd resin, 3 or 6% of wbop of active surfactant, 4% wbm (weight based on monomer) of stearyl acrylate, and $NaHCO_3$ at a concentration of 0.039 M in the water phase. To produce the miniemulsions, the organic and the aqueous phases were mixed by magnetic stirring (10 min at 1000 rpm), and the resulted mixture was sonified with a Branson 450 equipment (15 min, power 9 and 80% duty cycle). Finally, the miniemulsion was further treated (6 cycles) with a high-pressure homogenizer (Niro-Soavi, NS1001L PANDA) using $4.1 \times 10^7$ Pa in the first valve and $4.1 \times 10^6$ Pa in the second stage valve.

### Polymerization

Polymerizations were carried out in batch in a 1 L jacketed glass reactor (except the one carried out at 110 °C, which was performed in a calorimetric reactor, RC1-Mettler) equipped with reflux condenser, stirrer, sampling device, and nitrogen inlet. The reaction temperature (70 °C) was set constant by controlling the temperature of the

fluid in the jacket by means of a thermostatic bath and a heat exchanger. The miniemulsion was added to the reactor and kept under stirring and nitrogen atmosphere (12–15 mL/min). When V59 was used as initiator, it was dissolved in the organic phase before the miniemulsification process. When the miniemulsion reached the reaction temperature, the aqueous solution of KPS was added into the reactor as a shot. In the case of redox initiators and for the reaction carried out at 110 °C, a 0.25% of the oxidant was injected as a shot when the reaction mixture reached the desired temperature and then both oxidant and reductant (when used) were fed. After the end of the feeding, a batch period was maintained.

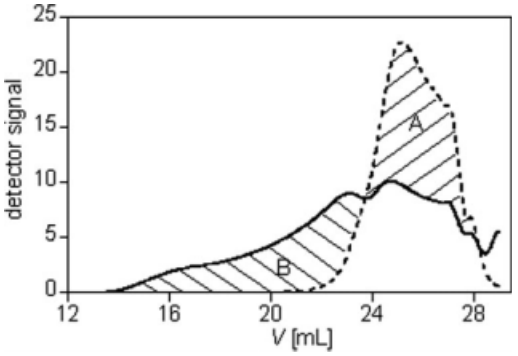


**Figure 1.** UV at 263 nm chromatogram of a hybrid sample (——) and of the alkyd resin S293 (– – –).

## Characterization

Conversion was measured by gravimetry. Droplet and particle sizes were determined by dynamic light scattering, using a Malvern Nanosizer, which provides a z-average diameter. It is worthy pointing out that in miniemulsion polymerization, dynamic light scattering does not allow distinguishing between monomer droplets and polymer particles. Therefore, after the start of the reaction, the reported values of the size of the dispersed phase were attributed to polymer particles.

The molecular architecture of the alkyd/acrylic hybrid latices was characterized by determining the fraction of alkyd resin grafted to the acrylic polymer (resin degree of grafting, RDG), the fraction of acrylic polymer grafted to the alkyd resin (acrylic degree of grafting, ADG), the fraction of double bonds of the alkyd resin consumed during the process, the gel content, and the sol molecular weight distribution (MWD).[20]

The sol fraction of the latex was separated from the gel fraction using soxhlet extraction. The filter with vacuum dried latex was placed inside a soxhlet, and the extraction was made using tetrahydrofuran (THF) under reflux during 24 h. The gel fraction, nonsoluble part, was determined as follows:

$$\text{Gel} = \frac{w_g}{w_p} \tag{1}$$

where $w_g$ and $w_p$ are the weights of the insoluble fraction and the whole sample, respectively.

The sol molecular weight distribution (MWD) and the mass fraction of alkyd resin grafted to the acrylic polymer (RDG) in the sol fraction were determined by Size Exclusion Chromatography (SEC). The SEC measurements were carried out with a LC-20AD Shimadzu pump fitted with a set of three fractionation columns (Waters Styragel HQ2, HQ4, HQ6) and two on-line detectors, a differential refractometer (DR) and a UV sensor (Waters) at 263 nm of wavelength. The RDG determination method was based on the fact that the acrylic polymer was not detected by the UV sensor at a wavelength of 263 nm. Therefore, the area of the baseline corrected UV-chromatogram of an acrylic/alkyd hybrid material was proportional to the resin concentration in the sol fraction of the sample. Figure 1 presents the UV signal of an acrylic/alkyd component (continuous line) and that of the neat alkyd resin (dash line). The areas of the two chromatograms were normalized so that they represented the same total area, that is, the same alkyd mass. The signal appearing at low elution volume ($V$) (i.e., high molecular weights) corresponded to the resin bounded to acrylic chains. Therefore, the areas of surfaces A and B were proportional to the amount of alkyd grafted to the acrylic polymer. The values of the areas A and B may be slightly different because double bonds of the alkyd resin could disappear during the grafting reactions. Consequently, for a given amount of alkyd resin, the UV signal of the hybrid polymer will be lower than that of the unreacted original alkyd resin. This means that the area A may be overestimated and the area B underestimated. An average of their values was obtained by making equal the area of the UV chromatogram of the hybrid sample to that of the original alkyd resin. In this way, the same values for the area $A$ and $B$ were obtained that corresponded to an estimation of the actual original value. Then, the RDG was estimated as: $A/A_{resin}$ or $B/A_{resin}$,

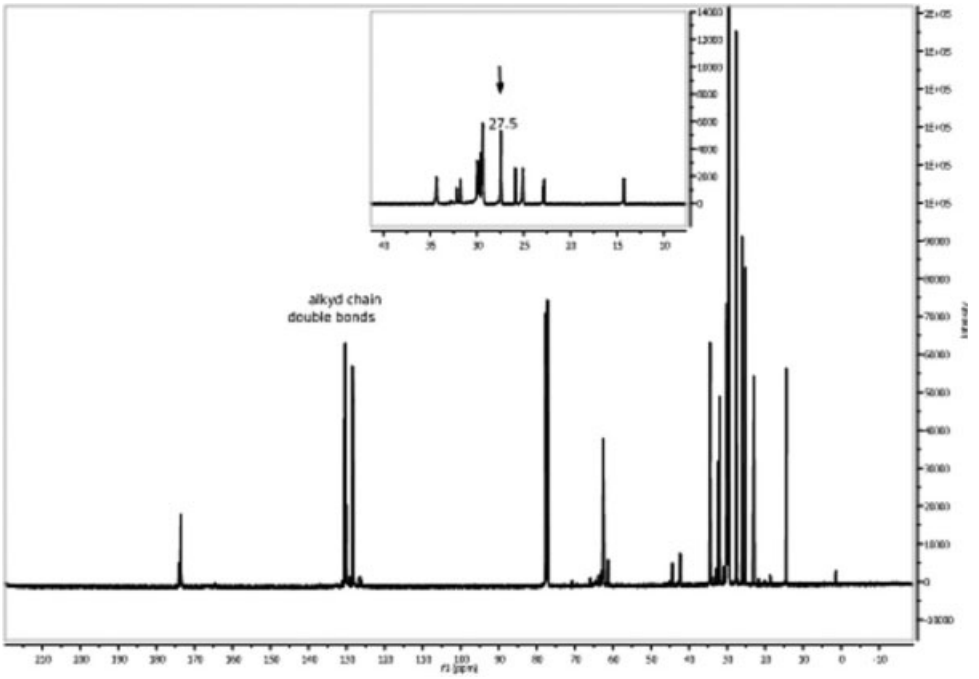


**Figure 2.** $^{13}$C-NMR spectra of alkyd resin with zoom at $\delta = 27.5$ ppm peak that remains unchanged.

where $A_{\text{resin}}$ is the area of the UV trace of the original resin (area below the dashed line in Fig. 1).

The MWD and the average molecular weights ($\overline{M}_n$ and $\overline{M}_w$) of the sol part were determined using the baseline corrected DR-chromatogram and a third order-direct calibration obtained with 20 narrow polystyrene standards in the range $10^3$–$10^6$. The MWD of the hybrids were very broad because they included the relatively high molecular weight acrylic polymer (both neat acrylic and alkyd grafted) and the low molecular weight ungrafted alkyd resin. The molecular weight distribution of the ungrafted alkyd resin was estimated by comparing the UV baseline-corrected chromatograms of the total hybrid sample and that of the original alkyd resin. Then, the MWD of the acrylic (grafted and neat) polymer without ungrafted resin was estimated.

The mass fraction of acrylic polymer that contained grafted alkyd resin defined as the acrylic degree of grafting (ADG), was determined by soxhlet extraction with diethyl ether. Filters containing the latex sample were dried in a vacuum oven at room temperature and weighed before and after the extraction. Although it has been reported that diethyl ether dissolves the free alkyd resin and the hybrid alkyd-acrylic components, but not the neat acrylic polymer,[8] it has been recently found that this ADG was overestimated because the solvent dissolved about a 25% of the neat acrylic polymer.[20] For high ADG values, the error is small, but substantial errors could be made at low ADG values.

The reacted double bonds of the resin were determined by $^{13}$C-NMR (Bruker Advance DPX 300). The region of interest in the spectrum is focused about 125–140 ppm, which corresponds to the double bonds of the resin (Fig. 2). The relative content of the reacted double bonds (RDB) was calculated using the following ratio.

$$\text{RDB} = 1 - [(A_{\text{double bonds}}/A_{xx})_{\text{hybrid}}/(A_{\text{double bonds}}/A_{xx})_{\text{resin}}] \times 100 \quad (2)$$

where $A_{\text{double bonds}}$ is the sum of the areas of the peaks of the double bond region, and $A_{xx}$ is the area of a reference peak of a methylene group of the resin (around 27.5 ppm) that remained unchanged in the alkyd during polymerization.

The morphology of latex particles was studied by means of transmission electron microscopy, TEM, using a TECNAI G$^2$ 20 TWIN (200 kV, LaB6). Five milliliters of a diluted dispersion of latex (solids content depending on particle size) was stained with 0.5 mL of a 4 wt % aqueous solution (in water) of osmium tetroxide. Samples were allowed to react during 7 days with the stain.

**Table 1.** Summary of Batch Miniemulsion Polymerizations Carried Out BA/MMA/AA (49.5/49.5/1); $T = 70$ °C

| Reaction | Resin Type | Initiator (% wbm) | Emulsifier Concentration (%) | $d_d$ (nm) | $d_p$ (nm) | $X$ (%) | $N_p/N_d$ |
|---|---|---|---|---|---|---|---|
| R1 | S293 | V59 (1.6) | 6 | 100 | 105 | 70 | 0.85 |
| R2 | S1630 | V59 (1.6) | 6 | 90 | 93 | 68 | 0.90 |
| R3 | S1630 | KPS (1.6) | 6 | 85 | 88 | 80 | 0.90 |
| R4 | S293 | V59 (1.6) | 3 | 123 | 124 | 57 | 0.97 |
| R5 | S293 | KPS (1.6) | 3 | 133 | 130 | 80 | 1.07 |
| R6 | S1630 | V59 (1.6) | 3 | 118 | 113 | 61 | 1.14 |
| R7 | S1630 | KPS (1.6) | 3 | 119 | 108 | 75 | 1.34 |

Positive staining with osmium tetroxide was used. $OsO_4$ reacts with double bonds of the resin, showing a dark image of the resin. Then, 0.1 mL of a 0.5% aqueous solution of phosphotungstic acid stain was added to each sample. The objective of this negative staining was to harden particles, and to increase electronic density in the surroundings of the particles and therefore the contrast. A drop of the stained diluted latices was placed on copper grids covered with formvar® (polyvinyl formal, Fluka) and dried at room temperature in a UV lamp. Micrographs were taken at different magnifications depending on particle size.

The interfacial tensions were measured by using an optical contact-measurement Dataphysics OCA 15 device.

## RESULTS

### Kinetics

Table 1 summarizes the experiments carried out in which the type of alkyd resin, the type of initiator and the emulsifier concentration (3 and 6% wbop) were varied. All reactions were carried out in batch at 70 °C. KPS is a water-soluble thermal initiator and the radicals are produced in the aqueous phase. V59 is a thermal oil-soluble initiator that produces the radicals inside the monomer droplets. Oil soluble initiators have been used in miniemulsion polymerization to limit diffusional degradation of the monomer droplets.[21] The main difference between the two alkyd resins used is their hydrophilicity. S293 is hydrophobic whereas S1630 is more hydrophilic.

Table 1 shows that the droplet size of miniemulsions prepared with 6% wbop of active emulsifier were smaller than those prepared with 3% of emulsifier. Furthermore, the droplet sizes of the miniemulsions prepared with the more hydrophilic alkyd resin (S1630) (runs R2, R3, R6, and R7) were smaller than those of the miniemulsions containing the hydrophobic alkyd resin (S293) (runs R1, R4, and R5).

Droplet size is given by the interplay between droplet break-up and coalescence.[22] For given homogenization conditions, droplet break-up depends on the viscosity of the organic phase and coalescence is governed by the miniemulsion stability. For the same organic phase and resin amount, the use of a higher emulsifier concentration improved the stability of droplets yielding smaller droplets size. With a 6% wbop of emulsifier, droplet sizes were around or below 100 nm, and with 3% wbop, the size was below 125 nm. This small effect of the emulsifier concentration on the droplet size shows that probably the maximum breaking capacity of the homogenization device was achieved, which limited the minimum size for this system.

On the other hand, the effect of the resin type on droplet size could be related to their hydrophobicity.[23] A higher hydrophobicity led to a stronger adsorption of the emulsifier on the droplet surface, which led to a higher surface coverage and lower emulsifier concentration in the aqueous phase. Therefore, droplet–droplet interaction increased leading to higher viscosity of the dispersed phase and hence a less intensive droplet break-up.[23] Coalescence was more likely for the hydrophobic resin because a higher hydrophobicity of the organic phase led to a higher demand of emulsifier for its stabilization. The combination of both factors resulted in smaller droplet sizes for the miniemulsions containing the hydrophilic resin.

It is worth pointing out that droplet sizes around and below 100 nm were obtained even though high solids contents and high resin

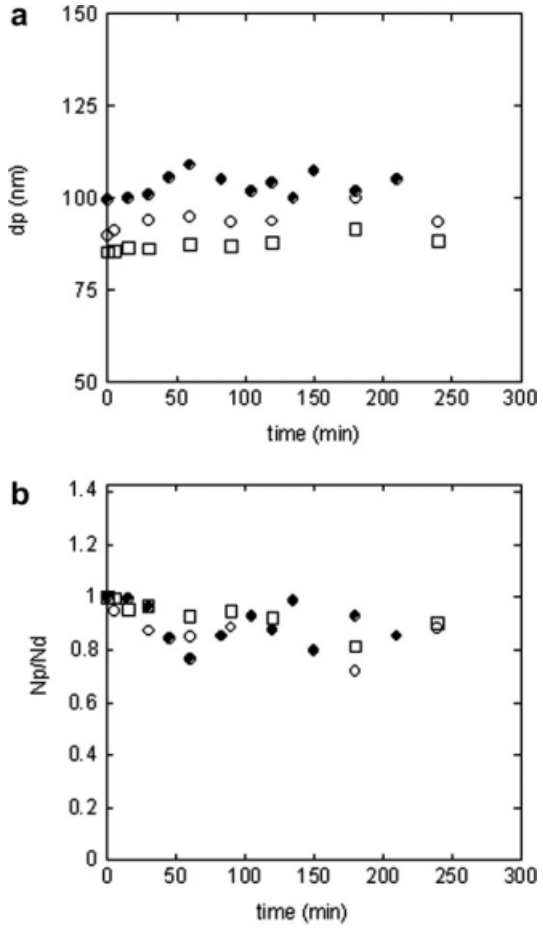


**Figure 3.** (a) Particle size evolution and (b) $N_p/N_d$ ratio evolution for latices produced with 6% surfactant (R1, ●; R2, ○; and R3, □).

contents were used. This is an improvement with respect to most of the reported studies in which larger droplets (200 nm) were obtained,[8] even when using low solids contents and a modest resin volume fraction (20%).[13,18] High solids contents offer numerous advantages for commercial applications[24,25] and low particles sizes facilitate ulterior film formation.[17]

Figures 3 and 4 show the evolution of particle size and the $N_p/N_d$ ratio during polymerization, when using 6 and 3% surfactant, respectively. It can be seen that in most cases, particle size remained relatively constant and close to the size of miniemulsion droplets during the whole process. This suggests that most of the droplets were nucleated and neither significant secondary nucleation nor coagulation occurred. Droplet nucleation is favored by the high stability of the miniemulsions.[26] Stable miniemulsion droplets can maintain their identity until they become polymer particles by either the entrance of one radical from the aqueous phase (when KPS is used) or by generation of a radical inside the droplet (when the oil-soluble V59 was used). The occurrence of secondary nucleation is less probable when oil-soluble initiators are used, but water-soluble initiators (e.g., KPS) yielding hydrophilic radicals are prone to form of new particles by homogeneous nucleation. The likelihood of this event is severely reduced by increasing the number of droplets in the system, that is, by using high solids contents and small particle/droplet sizes, as in the present case.[27]

Figure 5 shows that monomer conversion reached a plateau (limiting conversion) toward the end of the process. Furthermore, Figure 5 illustrates that the polymerization rate was faster when KPS (R3 and R5) was used and that the type of resin did not have a significant effect on the polymerization rate. The decomposition rate of KPS is slower than that of V59 ($1.5 \times 10^{-5}$

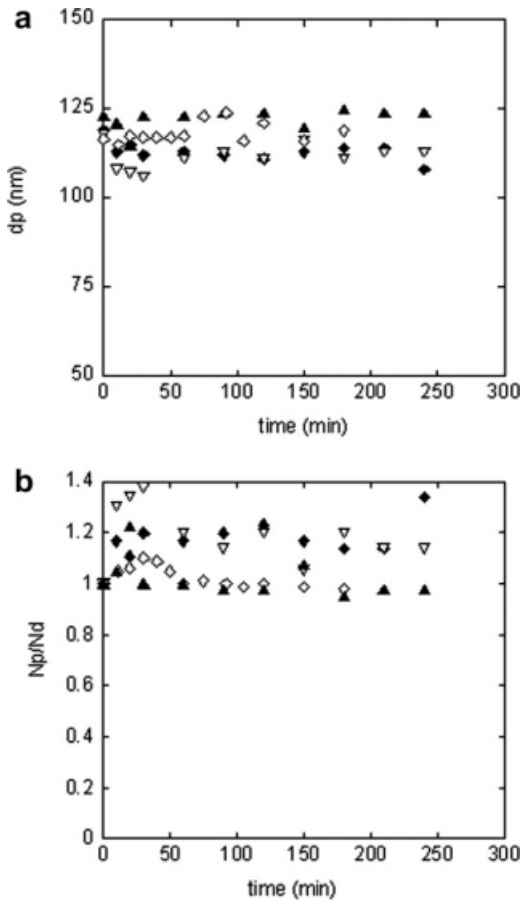


**Figure 4.** (a) Particle size evolution and (b) $N_p/N_d$ ratio evolution for latices produced with 3% surfactant (R4, ▲ R5, ◇; R6, ▽; and R7, ◆).

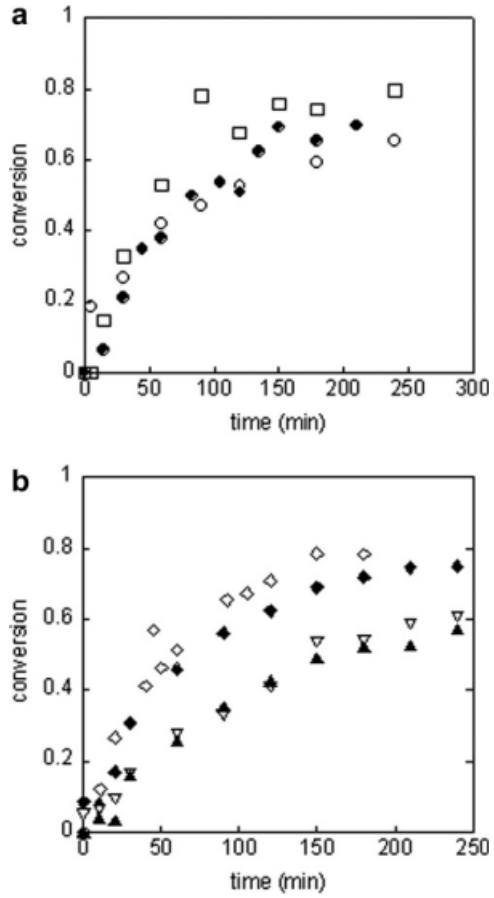


**Figure 5.** Acrylics conversion evolution. (a) latices produced with 6% surfactant (R1, ●; R2, ○; and R3, □), (b) latices produced with 3% surfactant (R4, ▲; R5, ◇; R6, ▽; and R7, ◆).

$s^{-1}$,[28] and $2.8 \times 10^{-5}$ $s^{-1}$,[29] at 70 °C, respectively). Therefore, the faster polymerization rate observed for KPS was due to the fact that the KPS derived radicals, which are produced in the aqueous phase are more efficient than the V59 derived radicals (produced inside the polymer particles), and therefore a large fraction of the latter ones undergo fast bimolecular termination.[30]

It is surprising that no effect of the number of particles on the polymerization rate was observed. The values of the average number of radicals per particle estimated using the values of the parameters given in Table 2 are very small ($\tilde{n} \ll 0.5$, see Table 3), and under these conditions (Case I Smith and Ewart[37]), the polymerization rate is independent of the number of polymer particles provided that radical termination in the aqueous phase is negligible

The values of $\overline{n}$ given in Table 3 are smaller than the values expected for particles of 90–130 nm.[37] The value of the desorption rate coefficient can be estimated from the Smith-Ewart Case I equation for $\overline{n}$.

**Table 2.** Values of the Parameters Taken From Literature; A: BA; B: MMA

| Parameter | Value/Reference |
|---|---|
| $k_{pA}$ | 2000–4000 (L/mol s)[31,32] |
| $k_{pB}$ | $1.06 \times 10^3$ (ref. 33) |
| $r_A$ | 0.31[34] |
| $r_B$ | 2.64[34] |
| $k_I$ | $1.5 \times 10^{-5}$ (ref. 28) |
| $f$ | 0.6 |
| $k_{tr}^{mon}$ BA | $7.41 \times 10^{-1}$ L/(mol s)[35] |
| $k_{tr}^{mon}/k_p$ MMA | $2.24 \times 10^{-2}$ L/(mol s)[36] |

$$\overline{n} = \frac{k_a[P_{tot}]_w}{2k_a[P_{tot}]_w + k_d} \quad (3)$$

where $k_a$ is the entry rate coefficient (L $mol^{-1}$ $s^{-1}$), $[P_{tot}]_w$ the concentration of radicals in the aqueous phase and $k_d$ ($s^{-1}$) is the desorption rate coefficient. For the range of values of $\overline{n}$ given in Table 3, $k_d \gg k_a [P_{tot}]_w$, and if radical termination in aqueous phase is negligible, then

$$k_a[P_{tot}]_w = 2fk_I[I]_w \frac{N_A V_w}{N_p} \quad (4)$$

where radical formation from a thermal water soluble initiator is considered and $f$ is the efficiency factor of the initiator radicals, $k_I$ the rate coefficient for initiator decomposition ($s^{-1}$), $[I]_w$ the concentration of the thermal initiator in the aqueous phase (mol $L^{-1}$), $N_A$ is the Avogadro's number and, $N_p$, the number of polymer particles in the reactor.

Using the values of the parameters in Table 2, the value of the exit rate coefficient estimated with eqs 3 and 4 was $k_d = 4.2$ $s^{-1}$. This value is substantially greater than the pseudo first order

**Table 3.** Average Number of Radicals per Particle

| Reaction | $\overline{n}$ |
|---|---|
| R1 | 0.04 |
| R2 | 0.03 |
| R3 | 0.03 |
| R4 | 0.04 |
| R5 | 0.09 |
| R6 | 0.05 |
| R7 | 0.05 |

**Table 4.** Summary of Miniemulsion Polymerizations with Initiator Feeding (MMA/BA/AA: 49.5/49.5/1)

| Reaction | Resin Type | Initiator (% wbm) | Polymerization Conditions ($T$) | $d_d$ (nm) | $d_p$ (nm) | $X$ (%) | $N_p/N_d$ |
|---|---|---|---|---|---|---|---|
| R8 | S293 | APS/MBS (1.6) | (70 °C), 4 h feeding, 2 h batch | 129 | 123 | 95 | 1.15 |
| R9 | S293 | APS/MBS (2.3) | (70 °C), 6 h feeding, 30 min batch | 145 | 134 | 97 | 1.27 |
| R10 | S293 | TBHP/AsAc (1.6) | (70 °C), 4 h feeding, 30 min batch | 147 | 133 | 89 | 1.35 |
| R11 | S293 | APS (1.6) | (110 °C), 4 h feeding, 1 h batch | 135 | 141 | 94 | 0.88 |

kinetic coefficient for production of monomeric radicals in the polymer particle by chain transfer to monomer, $k_{tr}^{mon}[M]_p = 6.1 \times 10^{-2}\ s^{-1}$, which means that chain transfer to monomer followed by desorption was not enough to justify the acute loss of radicals. Therefore, a radical sink should be present in the particles to account for the low values of $\overline{n}$. Probably, the alkyd resin acted as radical sink.

BA terminated radicals (and in a lesser extent MMA terminated radicals) are able to abstract the $\alpha$-hydrogen from the alkyd chain yielding an allylic radical that is rather unreactive because it is stabilized through delocalization in the $\pi$ system of the double bond.[3] This radical may undergo a termination (by combination) causing a further reduction of the number of radicals (as well as an increase in grafting). BA radicals may also attack the double bonds by direct addition forming a radical that, although more reactive than the allylic one produced by chain transfer, is less reactive than the acrylate radical. Because of the steric hindrance, the MMA terminated radicals are not expected to react with the double bonds of the alkyd resin.

These mechanisms may also be the reason for the observed limiting conversion. However, Tsavalas et al.[14] also proposed that the limiting conversion may be due to segregation of the resin within the polymer particle which resulted in alkyd-rich regions in which the acrylic radical cannot enter, and consequently, the monomer solubilized in those alkyd-rich domains cannot react. For the methyl methacrylate-alkyd system, Hudda et al.[15] concluded by simulation that retardative chain transfer was not capable of producing the limiting conversion, and that phase segregation was the most likely cause of the limiting conversion. However, it has been reported that complete conversion was achieved during the polymerization of acrylic monomer-alkyd dispersions in the presence of preformed acrylic latex.[38] This seems to challenge the segregation model because it shows that monomer may diffuse not only out of the segregated resin but also through the aqueous phase to the alkyd free particles. Rodriguez et al.[16] studied the limiting monomer conversion phenomenon occurring in the high solids silicone-modified acrylic miniemulsion polymerization. Experiments carried out with nonreactive PDMS did not present limiting conversion showing that this phenomenon was not due to monomer retention by the segregated PDMS. Propagation of BA radicals to the vinyl group of the reactive PDMS, which yielded very stable radicals, was likely the cause of the limiting conversion. Complete conversion was achieved by postpolymerization with redox initiators as well as by using a semicontinuous process with monomer feed.

In an attempt to achieve high monomer conversions during the polymerization of acrylic monomers in the presence of alkyd resins, higher reaction temperatures, redox initiators, and longer initiator feeding times were used (Table 4). R11 was carried in a calorimetric reactor (RC1-Mettler) under pressure.

Figure 6 presents the evolution of monomer conversion in the reactions summarized in Table 4. Comparison with Figure 4 shows that a substantial increase of the conversion was achieved using redox initiators or higher reaction temperature. Longer feeding times of the initiator

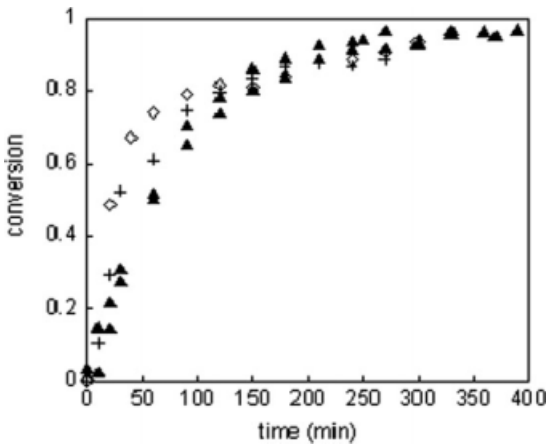


**Figure 6.** Acrylics conversion evolution of (R8, ▲; R9, ▲; R10, +; and R11, ◇).

**Table 5.** Effect of Process Conditions on Polymer Architecture: (a) Whole Polymer and (b) Acrylic Polymer

| Exp. | Gel (%) | $\overline{M}_{n,\mathrm{sol}}$ (g/mol) (a)/(b) | $\overline{M}_{w,\mathrm{sol}}$ (g/mol) (a)/(b) | ADG (%) | RDG (%) | RDB (%) |
|---|---|---|---|---|---|---|
| R1 | 0 | 4600/34,000 | 59,200/127,900 | 87 | 27 | 16 |
| R2 | 0 | 3532/32,600 | 48,654/102,700 | 30–50 | 13 | 5 |
| R3 | 0 | 3886/25,900 | 42,909/79,700 | 40–60 | 9 | 6 |
| R4 | 0 | 4200/32,800 | 34,300/79,600 | 90 | 14 | 12 |
| R5 | 0 | 4300/31,400 | 179,000/331,900 | 88 | 22 | 10 |
| R6 | 0 | 3500/32,660 | 50,300/102,700 | 30–50 | 14 | 13 |
| R7 | 0 | 3700/25,900 | 40,100/79,700 | 30–50 | 10 | 5 |
| R8 | 0 | 4000/30,600 | 110,800/216,100 | 97 | 17 | 4 |
| R9 | 1.5 | 5700/40,900 | $>3 \times 10^6$ | – | 39 | 14 |
| R10 | 0 | 3800/25,100 | 250,300/479,000 | – | 31 | 2 |
| R11 | 0 | 5800/34,700 | 129,756/297,600 | 95 | 29 | 5 |

(runs 8 and 9) also resulted in higher monomer conversions. The final conversion achieved with TBHP/AsAc was lower than that for APS/MBS (runs 8 and 10). TBHP/AsAc is interesting as TBHP partitions among the organic and the water phases (at 20 °C the partition coefficient octane/water is $P_{\mathrm{OW}} = 5$)[39] while AsAc remains in the aqueous phase. For this system, two sources of radicals are possible: thermal decomposition of the TBHP within the particles and redox reaction between TBHP and AsAc in the aqueous phase. The thermal decomposition rate of TBHP is very low ($10^{-10}$ $s^{-1}$ at 70 °C).[40] Therefore, the contribution of thermal initiation was negligible. Consequently, radicals were produced by a redox reaction in the aqueous phase. These are oxygen-centered hydrophobic radicals (very efficient in hydrogen abstraction), which enter directly into the particles, where they may abstract α-hydrogens from the alkyd chain yielding nonreactive radicals, namely reducing the polymerization rate. This hypothesis is further support by the high value of the RDG found in this experiment (Table 5). Another possible reason for the lower polymerization rate might be the diffusion of the TBHP to the polymer particles, which resulted in a TBHP/AsAc ratio different to the stoichiometric ratio of 2/1.[41] Under these circumstances, a reduction of radical production is expected.

## Polymer Structure

Table 5 presents the values of the gel content, resin and acrylic degrees of grafting (RDG and ADG), reacted resin double bonds (RDB), and average molecular weights ($\overline{M}_{\mathrm{n}}$ and $\overline{M}_{\mathrm{w}}$). For the average molecular weights, two values are given, one (a) corresponding to the total sample (i.e., including the free alkyd resin) and the other one (b) corresponding to the acrylic (neat and grafted) polymer.

Table 5 shows that no gel or very low amount of gel was obtained, which is agreement with the results reported by González et al.,[42] who found that no gel was formed in the copolymerization of BA and MMA, for MMA contents greater than 25%.

The molecular weights of the whole sample were low and the polydispersity index very high. However, these results are deceiving as they correspond to the whole polymer, namely, the pure acrylic polymer, the grafted acrylic-alkyd and the alkyd resin that was not grafted to the acrylic polymer. Table 5 also includes the values of the average molecular weights of the acrylic polymer (pure + grafted). Although these values are higher than those of the whole sample, they are relatively low for acrylic polymers produced in a compartmentalized system, further supporting the hypothesis that a strong chain transfer to the alkyd resin occurred.

For the hydrophobic resin (R1, R4, R5, and R8–R11), the choice of the initiator system had a strong effect on the molecular weight of the acrylic polymer. The thermal oil-soluble initiator V59 (R1 and R4) gave the smaller molecular weight because this initiator generates radicals in pairs within the droplets resulting in a severe bimolecular termination. Higher molecular weights were obtained when radicals were produced in the aqueous phase (KPS (R5), APS (R11); APS/MBS (R8); and TBHP/AsAc (R10)). Long process times (R9) led to very high molecular weights, likely because of the extensive chain transfer to the acrylic polymer chain resulting from the long exposure of the acrylic chains to the

radicals.[43] Chain transfer to polymer may also be the reason for the differences in molecular weights among the initiator systems yielding radicals soluble in the aqueous phase. Thus, TBHP/AsAc yielded higher molecular weights because this system produces oxygen centered hydrophobic radicals in the aqueous phase able to enter directly into the polymer particles. These radicals are very efficient for hydrogen abstraction, which increases the molecular weight by forming branches. The low amount of double bonds consumed in this case, indicates also that the abstraction of allylic hydrogen was important because contrary to addition mechanism, double bonds are not consumed in this mechanism.

For the KPS, the molecular weights obtained with the hydrophilic resin (R3 and R7) were smaller than those obtained with the hydrophobic one (R5). The reason may be that as the hydrophilic resin was located at the outer part of the resin (see the particle morphology section), it was more exposed to attack by both the carbon-centered entering radicals, formed by polymerization of sulfate ion radical with the monomer dissolved in the aqueous phase, and by the oxygen-centered sulfate ion radicals. For the oil soluble V59 (R2 and R6), the effect of the type of resin was modest.

Interestingly, the RDG was low for the hydrophilic resin (R2, R3, R6, and R7). This may be due to the low monomer concentration in the outer layers of the particles, which reduced the probability of formation of acrylic long branches by propagation of the allylic radicals. In addition, termination of these radicals with the short oligoradicals entering into the polymer particle would not give any measurable grafting.

By its chemical nature, S1630 may be more prone to suffer hydrogen abstraction than S293. A commonly used anhydride to improve alkyd water solubility is trimellitic anhydride.[44] The hydrogen from the carboxylic group of the anhydride can be easily abstracted forming a very stable radical in the alkyd chain. This could further contribute to explain both the lower molecular weight achieved with the hydrophilic resin and the lower resin grafting.

Table 5 shows that most of the acrylic polymer chains contained some grafted alkyd, whereas only a minor fraction of the alkyd was incorporated to the acrylic polymer. This difference is simply a matter of statistics. To illustrate this point, let us assume that the average molecular weight of the acrylic chain is 200,000 g/mol and

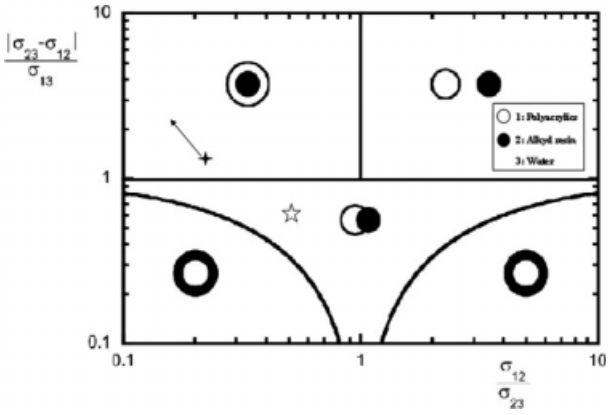


**Figure 7.** Diagram of thermodynamic equilibrium morphologies.

that of the alkyd resin is 10,000 g/mol, that is, there were 20 alkyd chains per acrylic chain. If 25% of the alkyd chains were grafted, as an average, each acrylic chain would have five grafted alkyd chains, namely, most of the acrylic polymer contained grafted alkyd chains, whereas 75% of the alkyd resin remained free.

Note that the ADG for R3 and R4 (hydrophilic resin) was given as a range. This is because for low values of ADG, the error of the technique is high, while above an 80% of ADG the error is negligible.[20] High values of ADG were obtained for the hydrophobic resin S293. In experiment R9, the acrylic degree of grafting could not be measured, because due to the high molecular weight of the polymer, a large fraction of the grafted polymer did not dissolve in diethyl ether. Run R10 was also affected by the same problem.

A higher resin degree of grafting was achieved when long process times or TBHP/AsAc was used. ADG, RDG, and RDB increased with temperature: When increasing reaction temperature (R11) conversion increased (Table 4) because both the rate of initiator decomposition and propagation rate augmented, which counteracted the increase of the chain transfer reaction mainly because of the high activation energy of the initiator decomposition.[35] The fraction of reacted double bonds was small in all cases, which ensured that a high amount of double bonds was available for the posterior curing process of the alkyd resin.

## Particle Morphology

Particle morphology is ruled by both thermodynamic and kinetic factors. The thermodynamic equilibrium morphology corresponds to the

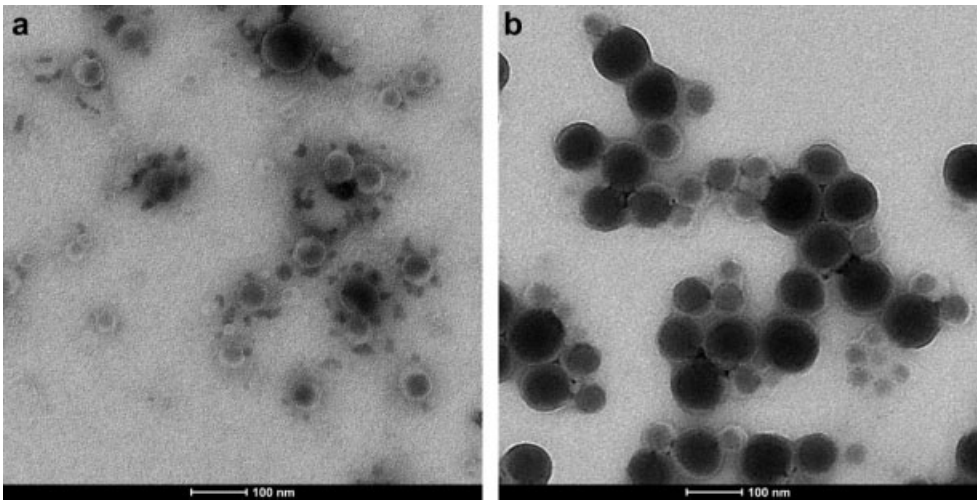


**Figure 8.** Particle morphologies observed by TEM of MMA/BA/AA (49.5/49.5/1)/S293 polymerized with different initiators. (a)V59 and (b) KPS.

minimum overall surface energy, which depends on the interfacial tensions.[45] For the hydrophobic resin, the interfacial tensions between polyacrylates (MMA/BA/AA: 49.5/49.5/1), alkyd resin SETAL 293, and aqueous phase measured were $\sigma_{12} = 10$ mN/m, $\sigma_{13} = 20$ mN/m, $\sigma_{23} = 33$ mN/m, respectively.

It is worth pointing out that these values corresponded to pure acrylic polymer and pure hydrophobic resin. Grafting should decrease the polymer-resin interfacial area ($\sigma_{12}$) and above a certain degree of grafting, it may affect the interfacial tensions between the polymer/water and resin/water. As relatively low values of RDG were found, it was not expected that $\sigma_{23}$ would be significantly affected by grafting. On the other hand, the actual value of $\sigma_{13}$ would likely be higher than that measured for the pure acrylic because almost all acrylic polymer contained grafted hydrophobic alkyd chains. Therefore, the values of the interfacial tensions measured with pure polymers were only indicative. The position of a system composed by pure acrylic polymer, and pure alkyd resin is represented by the black star in Figure 7. It can be seen that core-shell equilibrium morphology (alkyd resin in the core) was predicted. Grafting should not significantly affect this conclusion because it would decrease $\sigma_{12}$ (moving the position in the direction given by the arrow). The increase in $\sigma_{23}$ is not expected to be strong as only

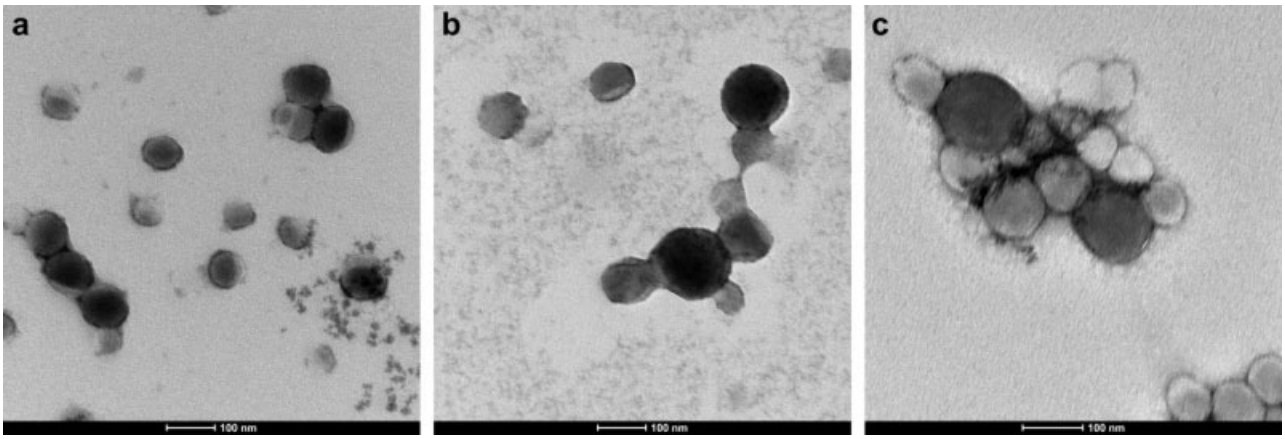


**Figure 9.** Particle morphologies observed by TEM of MMA/BA/AA (49.5/49.5/1)/S293 polymerized with different initiators. (a) APS/MBS 1.6% wbm, (b) APS/MBS 2.3% wbm, and (c) TBHP/AsAc.

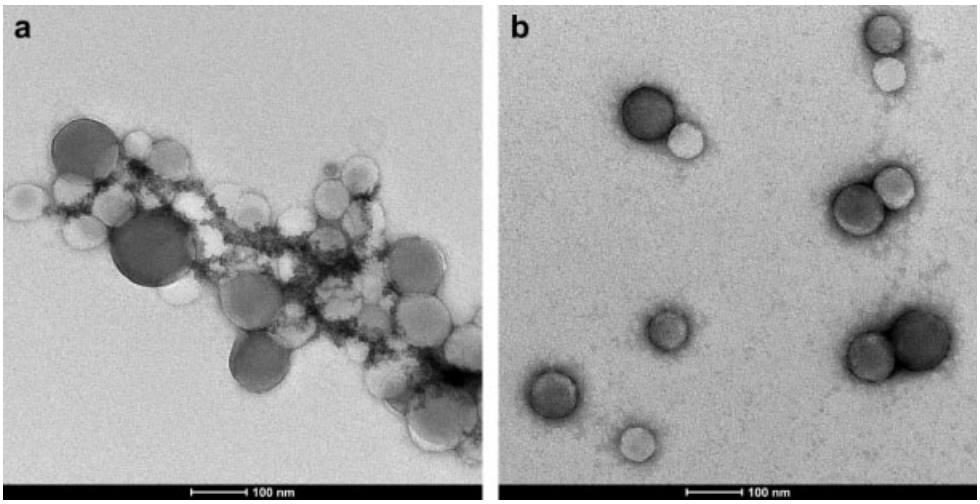


**Figure 10.** Particle morphologies observed by TEM of MMA/BA/AA (49.5/49.5/1)/ S293, APS 110 °C.

a maximum of 40% of the alkyd resin was grafted to acrylic polymer.

The predictions agree with the TEM micrographs shown in Figure 8, in which an alkyd rich dark core and acrylic lighter shell are observed. In addition, no strong effect of the initiator on particle morphology was observed which was in agreement with the similar grafting levels (ADG and RDG) achieved. The fact that equilibrium morphologies were achieved indicates that phase migration was relatively rapid in the system,[46] which is in agreement with the low viscosity in the polymer particles caused by the presence of the low molecular weight nongrafted alkyd resin and the relatively low molecular weight of the acrylic polymer.

Figure 9 shows the TEM micrographs of latices R8, R9, and R10. R8 had a high ADG but a very low resin degree of grafting and phase separation was evident. R9 and R10 presented the higher RDG and more homogeneous particles were observed.

Figure 10 shows particle morphology of R11 in which APS was fed at 110 °C. A relatively high RDG (29%) was obtained in this case. A very heterogeneous sample was achieved in which homogenous, core-shell, and homoacrylic particles can be observed. Although $N_p/N_d$ was lower than 1, Figure 10 suggests that homogenous nucleation occurred in some extent.

Based on these results one may speculate that a key parameter determining phase separation

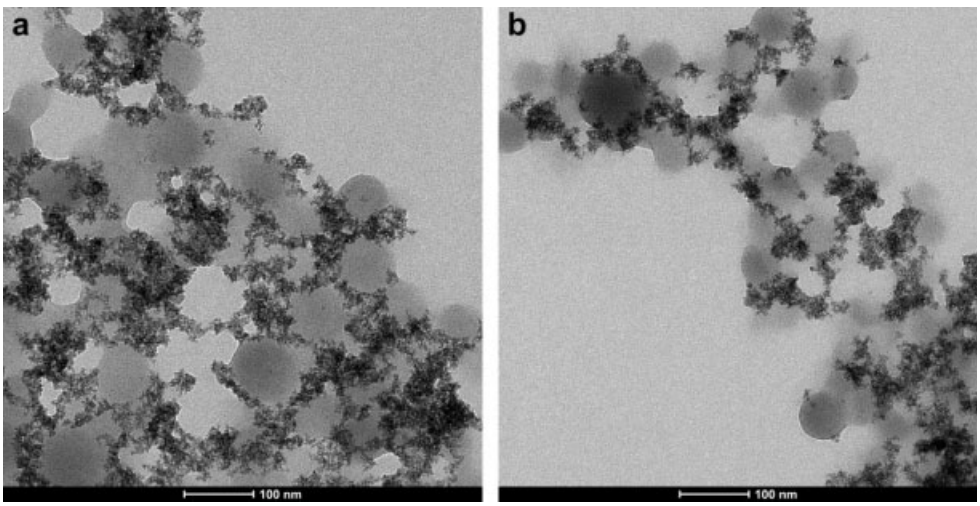


**Figure 11.** Particle morphologies of (a) MMA/BA/AA (49.5/49.5/1)/ S1630, V59 and (b) MMA/BA/AA (49.5/49.5/1)/ S1630, KPS.

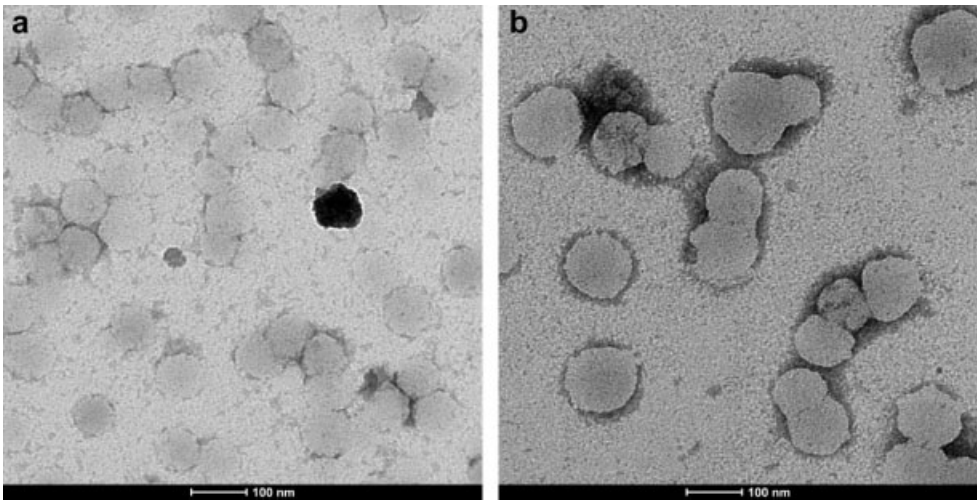


**Figure 12.** TEM images of stained blank latices (MMA/BA/AA/stearyl acrylate).

was the amount of resin grafted to acrylic. RDG influenced morphology more than ADG. The maximum RDG value achieved in this work was not enough to obtain a majority of homogenous hybrid particles.

When the hydrophilic alkyd resin (S1630) was used, no phase separation within the polymer particles was observed (Fig. 11). The TEM pictures show very small dark spots around the particles. To check if the dark spots were artifacts due to the staining procedure or the emulsifier, blank latices made with the same emulsifier type and amount and the same acrylic composition were subjected to the same staining procedure. The TEM images (Fig. 12) did not show dark spots, and therefore it can be concluded that the dark spots were not stained emulsifier or unreacted $OsO_4$. Therefore, it was supposed that the dark spots were segregated alkyd or soluble parts of the resin.

For the hydrophilic resin, using the values of the interfacial tensions ($\sigma_{12} \sim 12$ mN/m and $\sigma_{23} \sim$ 25–30 mN/m, $\sigma_{13} \sim 20$ mN/m), Thermodynamics predicts that a hemispheric morphology (white star in Fig. 7) should be reached at equilibrium. Therefore, what is observed in the TEM pictures may be the result of a hemispherical morphology which lost the mechanically weak alkyd part during sample preparation.

## CONCLUSIONS

The kinetics of the miniemulsion polymerization used to synthesize high solids content waterborne acrylic-alkyd nanocomposites and the effect of process conditions on polymer architecture and particle morphology was studied.

The use of thermal initiators in the range of temperatures commonly used in polymerization in dispersed media (70 °C) led to limiting conversion. Alkyd resin was found to act as a radical sink due to chain transfer to alkyd, which forms a rather unreactive radical stabilized by the conjugation of the double bond. The hydrophobicity of alkyd resin did not affect the polymerization kinetics. High monomer conversions were achieved using higher reaction temperatures for thermal initiator (110 °C) and redox initiators, in semicontinuos.

For the hydrophobic resin, initiators yielding radicals in the aqueous phase (KPS, APS, APS/MBS, TBHP/AsAc) led to higher molecular weights than the oil-soluble initiator (V59), likely because in this case, radicals are produced in pairs within the particles resulting in a severe bimolecular termination. TBHP/AsAc yielded particularly high molecular weights by forming branches through hydrogen abstraction.

For the KPS, the molecular weights obtained with the hydrophilic resin were smaller than those obtained with the hydrophobic one. The location of the hydrophilic resin at the outer part of the particles, where it is more accessible to the radicals, may be reason for the difference. The chemical nature of S1630 may also contribute to this effect.

Most of the acrylic polymer chains contained some grafted alkyd, whereas only a fraction of the alkyd was incorporated to the acrylic polymer.

The values of ADG, RDG, and the fraction of reacted double bonds were considerably lower for the hydrophilic resin than those for the hydrophobic resin.

For the hydrophobic resin, core-shell morphologies were clearly observed. The use of long feeding times, TBHP/AsAc and higher reactions temperatures for thermal initiators increased the degree of resin grafting, yielding more homogenous particles. When the hydrophilic resin was used, an important part of the alkyd resin appeared in the TEM micrographs outside the polymer particles. However, this may be the result of a hemispherical morphology which separated during sample preparation.

The financial support received from the European Union project (Napoleon NMP3-CT-2005-011844) is gratefully appreciated.

## REFERENCES AND NOTES

1. Van Haveren, J.; Oostveen, E. A.; Micciché, F.; Noordover, B. A. J.; Koning, C. E.; van Benthem, R. A. T. M.; Frissen, A. E.; Weijnen, J. G. J. J Coat Technol Res 2007, 4, 177–186.
2. Directive 2004/42/CE of the European Parliament and the Council, Official J of the European Union.
3. Nabuurs, T.; Baijards, R. A.; German, A. L. Prog Org Coat 1996, 27, 163–172.
4. Wang, S. T.; Schork, F. J.; Poehlein, G. W.; Gooch, J. W. J Appl Polym Sci 1996, 60, 2069–2076.
5. Ugelstad, J.; El-Aasser, M. S.; Vanderhoff, J. W. J Polym Sci: Polym Letters Ed 1973, 11, 503–513.
6. Antonietti, M.; Landfester, K. Prog Polym Sci 2002, 27, 689–757.
7. Asua, J. M. Prog Polym Sci 2002, 27, 1283–1346.
8. Wu, X. Q.; Schork, F. J.; Gooch, J. W. J Polym Sci Part A: Polym Chem 1999, 37, 4159–4168.
9. Van Hamersveld, E. M. S.; Van Es, J.; Cuperus, F. P. Colloids Surf A 1999, 153, 285–296.
10. Van Hamersveld, E. M. S.; Van Es, J. J. G. S.; German, A. L.; Cuperus, F. P.; Weissenborn, P.; Hellgren, A. C. Prog Org Coat 1999, 35, 235–246.
11. Monteiro, M. J.; Subramaniam, N.; Taylor, J. R.; Pham, B. T. T.; Tonge, M. P.; Gilbert, R. G. Polymer 2001, 42, 2403–2411.
12. Huang, N. J.; Sundberg, D. C. J Polym Sci Part A: Polym Chem 1995, 33, 2553–2549.
13. Tsavalas, J. G.; Luo, Y.; Schork, F. J. J Appl Polym Sci 2003, 87, 1825–1836.
14. Tsavalas, J. G.; Luo, Y.; Hudda, L.; Schork, F. J Polym React Eng 2003, 11, 277–304.
15. Hudda, L.; Tsavalas, J.; Schork, F. J. Polymer 2005, 46, 993–1001.
16. Rodriguez, R.; Barandiaran, M. J.; Asua, J. M. Polymer 2008, 49, 691–696.
17. Keddie, J. Mater Sci Eng Reports 1997, 21, 101–170.
18. Tsavalas, J. G.; Schork, F. J.; Landfester, K. JCT Research 2004, 1, 53–63.
19. Guo, J.; Schork, F. J. Macromol React Eng 2008, 2, 265–276.
20. Minari, R.; Goikoetxea, M.; Beristain, I.; Paulis, M.; Barandiaran, M. J.; Asua, J. M. J Appl Polym Sci, in press. (Molecular Architecture of Alkyd/Acrylic Latexes Prepared by Miniemulsion Polymerization).
21. Alduncin, J. A.; Forcada, J.; Asua, J. M. Macromolecules 1994, 27, 2256–2261.
22. Manea, M.; Chemtob, A.; Paulis, M.; de la Cal, J. C.; Barandiaran, M. J.; Asua, J. M. AIChE J 2008, 54, 289–297.
23. López, A.; Chemtob, A.; Milton, J. L.; Manea, M.; Paulis, M.; Barandiaran, M. J.; Theisinger, S.; Landfester, K.; Hergeth, W. D.; Udagama, R.; McKenna, T.; Simal, F.; Asua, J. M. Ind Eng Chem Res 2008, 47, 6289–6297.
24. Guyot, A.; Chu, F.; Scheneider, C.; Graillat, C.; McKenna, T. F. Prog Polym Sci 2002, 27, 1573–1615.
25. do Amaral, M.; van Es, S.; Asua, J. M. Macromol Theory Simul 2004, 13, 107–114.
26. Rodriguez, R.; Barandiaran, M. J.; Asua, J. M. Macromolecules 2007, 409, 5735–5742.
27. Ferguson, C. J.; Russel, G. T.; Gilbert, R. G. Polymer 2002, 43, 4557–4570.
28. Kolthoff, J. M.; Miller, I. K. J Am Chem Soc 1951, 73, 3055–3059.
29. Waco Pure Chem. Azo polymerization Initiators product information.
30. Autran, C.; de la Cal, J. C.; Asua, J. M. Macromolecules 2007, 40, 6233–6238.
31. Asua, J. M.; Beuermann, S.; Buback, M.; Castignolles, P.; Charleux, B.; Gilbert, R. G.; Hutchinson, R. A.; Leiza, J. R.; Nikitin, A. N.; Vairon, J. P.; van Herk, A. Macromol Chem Phys 2004, 205, 2151–2160.
32. Asua, J. M. J Polym Sci Part A: Polym Chem 2004, 42, 1025–1041.
33. Beuermann, S.; Buback, M.; Davis, T. P.; Gilbert, R. G.; Hutchinson, R. A.; Olaj, O. F.; Russell, G. T.; Schweer, J.; Van Herk, A. M. Macromol Chem Phys 1997, 198, 1545–1560.
34. Bandrup, J.; Immergut, H. Polymer Handbook; Wiley: New York, 1975.
35. Hutchinson, R. A.; Penlidis, A. In Polymer Reaction Engineering; Asua, J. M., Ed.; Blackwell: Oxford, 2007; Chapter 3, pp 118–178.
36. Achilias, D. S.; Kiparissides, C. Macromolecules 1992, 25, 3739–3750.
37. Smith, W. V.; Ewart, R. H. J Chem Phys 1948, 16, 592–599.

38. Overbeek, G. C.; Scheerder, J.; Steenwinkel, P.; Tennebroek, R. WO 02/28977 A2; April 11, 2002.
39. Van Hooidink, C. TNO Report 1992 PML 1992-C26 TNO Prins Maurits laboratory, Rijswijk, The Netherlands.
40. Peck, N. F. A.; Asua, J. M. Macromolecules 2008, 41, 7928–7932.
41. Da Cunha, L.; Ilundain, P.; Salazar, R.; Álvarez, D.; Barandiaran, M. J.; Asua, J. M. Polymer 2001, 42, 391–395.
42. González, I.; Asua, J. M.; Leiza, J. R. Polymer 2007, 48, 2542–2547.
43. González, I.; Asua, J. M.; Leiza, J. R. Macromolecules 39, 2006, 5015–5020.
44. Amoco Chemicals Corp., Tech. Bull. TMA-1086, 1981.
45. González-Ortiz, L. J.; Asua, J. M. Macromolecules 1995, 28, 3135–3145.
46. González-Ortiz, L. J.; Asua, J. M. Macromolecules, 1996, 29, 4520–4527.